

SIMULATION OF A PERPENDICULAR BOW SHOCK

M. M. Leroy, C. C. Goodrich, D. Winske, C. S. Wu and K. Papadopoulos

University of Maryland, College Park, MD, 20742

Abstract

Simulations of a high Mach number shock with parameters typical of the earth's bow shock have been performed using a hybrid (particle ions, fluid electrons) code. The simulations reproduce the observed ion reflection and overshoots in the magnetic field and density. These features are shown to be closely associated with ion gyration.

Introduction

The purpose of this letter is to report preliminary results obtained from numerical simulations of a high Mach number magnetosonic shock wave. The present study is motivated by recent ISEE spacecraft observations of the Earth's bow shock. Particularly interesting features of the quasi-perpendicular bow shock include:

(i) Ion reflection

The density of the reflected ions appears to be surprisingly large, approximately 20% of the solar wind density (Paschmann *et al.*, 1981). Furthermore, the observations suggest that these ions eventually reach the downstream region without thermalizing rapidly. They contribute, however, very significantly to the pressure balance in the downstream region.

(ii) Magnetic field overshoot

The magnetic field in the shock transition layer has been found to exhibit a rather complicated overall structure, including very frequently a foot region, a sharp ramp, and an extended overshoot. The presence of a magnetic field overshoot was first pointed out by Heppner *et al.* (1967) and has been discussed more recently by Russell and Greenstadt (1979), Bame *et al.* (1979), and Russell *et al.* (1981).

(iii) Size of the overall shock transition layer

The use of two different spacecraft in the ISEE mission has allowed reliable determinations of the length scales that characterize the shock transition layer (Russell and Greenstadt, 1979). The overall structure has been found to extend over hundreds of kilometers, which is equivalent to many ion inertia lengths (c/ω_{pi}) or more relevantly, as shown below, to a few ion gyroradii. The electron inertia length c/ω_{pe} is much smaller, only about 2 km. In contrast, theoretical studies of collisionless perpendicular shock waves have considered c/ω_{pe} or resistive scale lengths as dominant lengths of the shock structure. This is indeed so for low

Mach number cases, whose laminar structures have been adequately described by magnetosonic wavetrains that scale as c/ω_{pe} (Tidman and Krall, 1971). Computer simulations, including both electron and ion scales, have significantly advanced the understanding of higher Mach number shocks, in which ion reflection occurs (Papadopoulos *et al.*, 1971; Forslund and Freidberg, 1971; Mason, 1972; Auer *et al.*, 1971; Biskamp and Welter, 1972). However, the large scale lengths ($\gg c/\omega_{pe}$) observed by the ISEE spacecraft strongly suggest that electron scales are not significant for the overall shock structure. In this paper, we use a simulation model in which electrons are considered as a massless fluid so that electron scales are neglected. This simplifies the numerical investigation of the large scales associated with ions but requires an artificial description of phenomena occurring on shorter scales (e.g., electron heating).

We consider here magnetized ions. The importance of magnetic effects for ion heating was first suggested by Auer *et al.* (1971) and Biskamp and Welter (1972), and further discussed by Sherwell and Cairns (1976), and Morse (1976). We have found that magnetic effects on ions are sufficient to form a quasi-stationary high Mach number shock structure, through a self-consistently sustained ion reflection process. This is in contrast to the results of Biskamp and Welter (1972), who found a highly oscillatory, nonstationary shock front. Furthermore, these magnetic effects are shown to lead to scale lengths and magnetic field overshoot consistent with observations.

Simulation Results

The simulations have been performed using a hybrid code in which the ions are treated kinetically using standard particle-in-cell techniques, while the electrons are treated as a massless, charge neutralizing fluid (Chodura, 1975; Sgro and Nielson, 1976). One spatial dimension x and all velocity and field components are included in the calculation. Dissipation is included in the form of a macroscopic phenomenological resistivity, which gives rise to Ohmic heating of the electrons.

The simulation is initialized with conditions that represent an idealized shock transition which is allowed to evolve in time in the shock rest frame. This initial state consists of two uniform regions separated by a step discontinuity. In the upstream state (the left region in the simulation), the particle ions are uniformly distributed in x and given random velocities to approximate a Maxwellian distribution convecting toward the discontinuity with appropriate density n_1 , temperature T_{i1} and flow speed V_{x1} . The upstream magnetic field B_1 (in the z direction) and temperature of the fluid

Copyright 1981 by the American Geophysical Union.

electrons T_{e1} are also assumed to be uniform. The downstream region is prepared similarly with appropriate density n_2 , ion temperature T_{i2} , flow speed V_{x2} , magnetic field B_2 , and electron temperature T_{e2} . These downstream quantities are computed from the upstream values using the Rankine Hugoniot relations (Tidman and Krall, 1971) and an assumed initial value of T_{e2}/T_{i2} . In order to take into account magnetic effects on the ions the system length is chosen to be much larger than an average ion gyroradius. The system is allowed to evolve in time and space with the magnetic field B fixed at the boundaries. A constant flux of upstream plasma is maintained at the left end, balanced by an equal flux of downstream plasma leaving the system at the right end. This implies that the total number of particles is conserved.

The simulation described here is initialized with the following upstream parameters: $n_1 = 8 \text{ cm}^{-3}$, $B_1 = 5 \text{ } \gamma$, $T_{e1} = T_{i1} = 4.7 \text{ eV}$, $V_{x1} = 304 \text{ km/s}$; the corresponding beta values are $\beta_e = \beta_i = 0.6$ and the Alfvén Mach number $M_A = 1.8$. Downstream the initial values are: $n_2 = 28.7 \text{ cm}^{-3}$, $B_2 = 18 \text{ } \gamma$, $V_{x2} = 78 \text{ km/s}$, $T_{e2} = T_{i2} = 86 \text{ eV}$. These parameters correspond to the preliminary results for the ISEE shock crossings of Nov. 7, 1977, as discussed at the CDAW-3 Workshop (June 23-25, 1979). This shock observation provides one of the most detailed

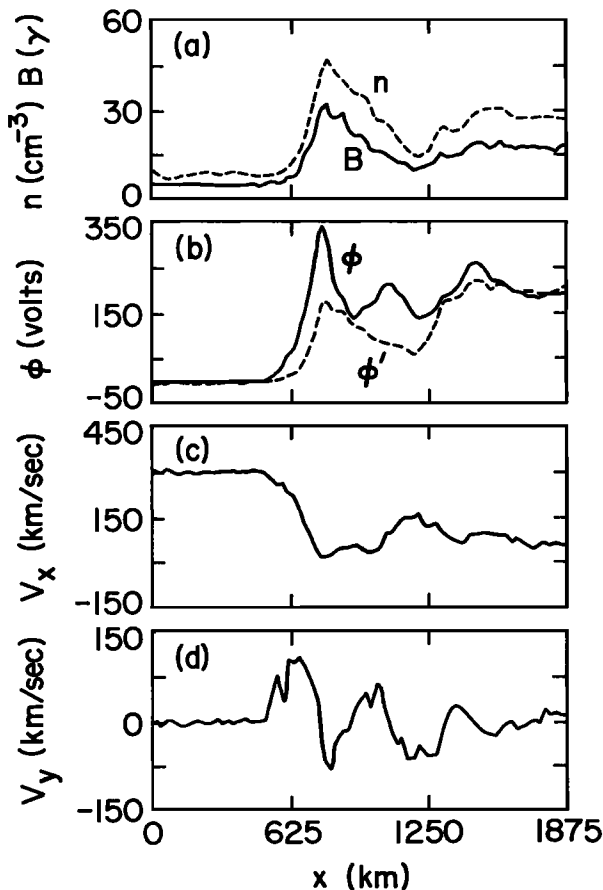


Fig. 1 - Profiles of shock quantities at $t = 8$ sec.; (a) B (solid line) and n (dashed line), (b) ϕ (solid line) and $\hat{\phi}$ (first term of Eq. (3) (dashed line) (c) V_x , and (d) V_y .

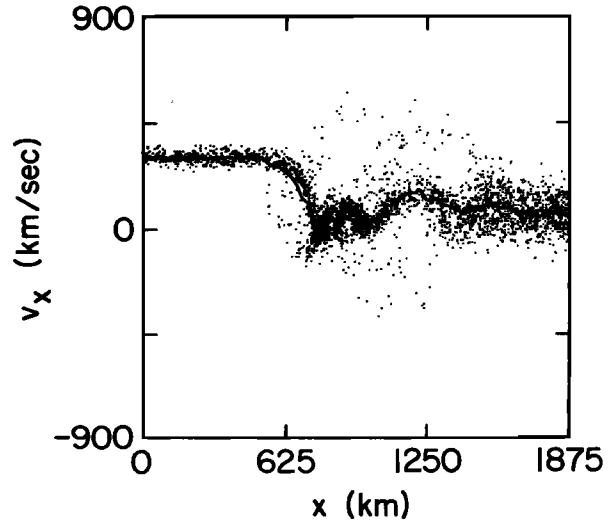


Fig. 2 - v_x versus x phase space at $t = 8$ sec.: solid curve is V_x .

data sets in existence for a quasi-perpendicular shock; in a future publication, detailed comparisons of the simulation results with observations will be presented. The purpose of this letter is to demonstrate that the simulation reproduces an overall shock structure generally consistent with the observations, and to clarify the operable physical processes.

After an initial transitory period lasting about a gyroperiod $\tau \approx 3$ sec (computed using the downstream magnetic field B_2), a self-sustained shock structure is produced and maintained. Results of the simulation, at a typical time $t = 8 \text{ sec} \approx 4 \omega_{ci}^{-1}$ (ω_{ci} is the upstream ion gyrofrequency) are presented in Fig. 1. Plotted are the spatial profiles of magnetic field, density, electric potential ϕ , and mean ion velocities V_x and V_y . We have used realistic rather than dimensionless units in Fig. 1 (B in γ , n in cm^{-3} , V_x and V_y in km/s , and x in km) to facilitate the comparison of our results with the ISEE observations. The magnetic field (Fig. 1a) exhibits the overall structure of the observations, including a foot region ($540 \text{ km} < x < 700 \text{ km}$), a magnetic ramp ($700 \text{ km} < x < 800 \text{ km}$) and a large, well-defined overshoot ($700 \text{ km} < x < 1100 \text{ km}$). While the density profile (dashed line in Fig. 1a) closely follows that of the magnetic field (since the resistivity is small), the potential profile does not (Fig 1b). A much narrower overshoot appears in the potential. Once established, the overall structure persists in time, although the plasma and field quantities do show small temporal oscillations over the ion gyroperiod τ . For example, the magnetic field overshoot B_{max}/B_2 varies by about 20% around its average value of 1.7. This is in contrast to previous simulations where the leading edge of the shock periodically vanishes (Biskamp and Welter, 1972).

Figures 2 and 3 present ion phase space at the same time. The v_x versus x phase space (Fig. 2) shows the upstream ions incident from the left slowed as they enter the shock region ($x = 540 \text{ km}$). The small number of particles with smaller x velocities in this region are ones which are reflected from the shock. These same particles

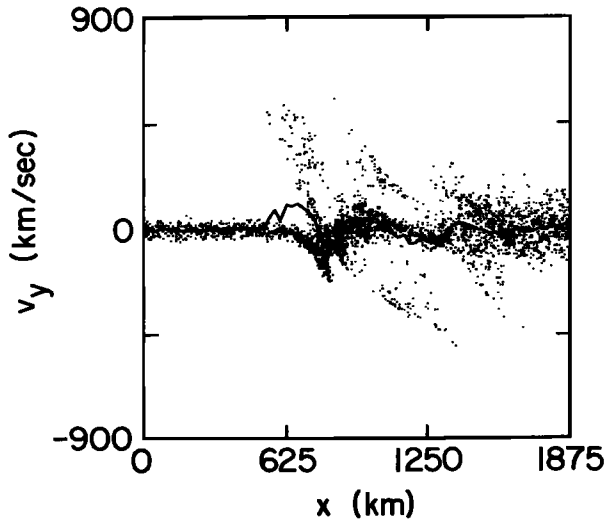


Fig. 3 - v_y versus x phase space at time $t = 8$ sec.; solid curve is V_y .

have large values of v_y (v_y versus x phase space, Fig. 3). The reflected particles constitute part of a gyrating stream, which can be seen in Fig. 2 by following the small group of particles starting at $x = 540$ km, below the main incident beam, upward to large v_x , and then across larger x (~ 900 km) at large v_x (~ 500 km/sec). The stream continues at $x \approx 1100$ km, starting at large v_x , continuing to negative v_x (at the same x), then upstream. Similarly, a second gyrating stream can be seen at larger x (starting at $x = 1100$ km). That these particles are gyrating is evident when comparing with Fig. 3. In regions where the gyrating particles have small v_x , they have large v_y and vice versa. The average gyroradius of these particles is about 300 km. This gyrating stream can be correlated with the overall structure of the shock by comparing Fig. 2 with Fig. 1a. The foot region of the magnetic field corresponds to the region of reflected particles in front of the shock, while the length of the overshoot of the magnetic field is roughly the gyroradius of the gyrating particles.

The presence of the gyrating ions results in non-thermalized ion distributions with large relative drifts (Auer *et al.*, 1971; Biskamp and Welter, 1972), which are consistent with observations (Greenstadt and Fredricks, 1979; Paschmann *et al.*, 1981). They also represent enough momentum flux to shift the ion rest frame in both v_x and v_y . This can be seen in the deviation of the solid lines in Figs. 2 and 3, which are the average ion velocity components, V_x and V_y respectively, from the portions of the main ion component. Most of the incident ions penetrate into the ramp region and are heated by compression. Note that the thermal spread of the ions in both the v_x and v_y phase space plots (Fig. 2 and 3) is much broader for $x > 1500$ km. This does not represent thermalization; rather, it is a remnant of the initial downstream plasma.

For these results the resistivity was constant and equal to 10^{-7} sec. This resistivity, though much larger than classical, is much smaller than the anomalous resistivity expected from cross field instabilities (Davidson and Krall, 1977). The overall structure of the shock (foot, ramp,

overshoot) is rather insensitive to the value of the resistivity; simulations in which we have varied the resistivity by two orders of magnitude produce similar results.

Discussion

The significant features of the simulation results, ion reflection, the potential overshoot, and the magnetic field overshoot, are associated with the gyrating ions. We note first from Figure 1b that ϕ reaches a maximum ϕ_{\max} of roughly 330 V. This rather large potential is itself due to ion gyration, as we discuss below. It is however insufficient to reflect any of the upstream ions, which have energies of approximately 480 eV.

A fraction of the incoming ions are reflected near the potential maximum because they are decelerated in the x direction by the Lorentz force in the foot region. The equations of motion for individual ions are

$$\frac{d}{dt} v_x = -\frac{e}{M} \frac{\partial}{\partial x} \phi + \frac{e}{Mc} v_y B \quad (1)$$

$$\frac{d}{dt} v_y = -\frac{e}{Mc} (v_x - V_x) B \quad (2)$$

where M is the ion mass and we have used

$E_y = V_x B/c$, which is approximately valid for the small value of resistivity assumed in our model. Figure 2 shows that the x velocities for the incoming ions are significantly larger than V_x in the foot region, due to the contribution to V_x of the reflected ions. The incoming ions thus acquire negative velocities in the y direction and are decelerated in the x direction, according to the above equations, so that some of them are reflected. This reflection process is self-sustaining. There must be sufficient reflected ions in the foot region to shift the ion rest frame. Then the incoming ions can be magnetically slowed enough so that a fraction of them can be reflected, continuing the process. The seed population of ions necessary to start the process is provided initially by transients that cause some of the downstream ions to flow upstream of the magnetic ramp. The details of the transitory period are strongly dependent on the initial value of T_{e2}/T_{i2} chosen. However, after this period, the resulting shock structure is found to be insensitive to this parameter.

The potential structure, shown in Fig. 1b, in particular the narrow overshoot, is due primarily to ion gyration. Under the assumption of quasi-neutrality ϕ may be obtained by neglecting the electron mass in the y component of the electron momentum equation:

$$e \phi(x) = \int_{-\infty}^x \frac{1}{n} \frac{\partial}{\partial x} \left(\frac{B^2}{8\pi} + nT_e \right) dx + \int_{-\infty}^x \frac{1}{c} v_y B dx \quad (3)$$

Contributions to the second term in this equation are due to the deflections of the net ion velocity in the y direction, shown in Fig. 1d, caused by the gyrating ions. This term is quite significant, as pointed out by Auer *et al.* (1971). Its magnitude can be estimated in Fig.

1b which shows profiles of ϕ (solid line) and a reduced potential ϕ' consisting of the first term in Eq. (3) (dashed line). The potential difference $\Delta\phi$, which is just the last term of Eq. (3), is quite large (200 volts maximum). $\Delta\phi$ is positive in the foot and ramp region ($540 \text{ km} < x < 800 \text{ km}$), because V_y is positive due to large y velocities of the gyrating ions. For larger x ($800 \text{ km} < x < 910 \text{ km}$), V_y is negative, being dominated by the population of ions which in transmitting the foot and ramp regions acquired negative y velocities as discussed above, while the velocities of the gyrating ions are predominantly in the x direction in this region.

The magnetic field overshoot can be qualitatively understood in terms of the ion trajectories by considering the density profile, since B/n is approximately constant. The incoming ions pile up in the foot and ramp regions as they are magnetically and electrostatically decelerated, with the density increasing to a maximum of 40 cm^{-3} at the position of the potential peak. These ions have negative y velocities (as discussed above), and are not greatly accelerated while flowing through the downstream side of the potential overshoot. As a result, the density remains large in this region.

The density overshoot is further enhanced by the gyrating ions. The downstream guiding center velocity of these ions is so small ($\sim 75 \text{ km/s}$) that, neglecting ϕ , they would return close to the ramp region one gyroperiod after being reflected. However, the potential overshoot prevents them from approaching the ramp region; they instead pile up at the downstream side of the potential hill ($x \approx 900 \text{ km}$). This extends the density and associated magnetic field overshoot width to roughly 400 km .

In conclusion, the simulation results are consistent with the observed overall structure within a typical perpendicular shock transition layer in the Earth's bow shock. Gyrating ions play a crucial role in building up and maintaining overshoots in the potential, density and magnetic field. The ion thermalization process, which is not included in our model, is observed to operate on a scale length larger than an ion gyroradius and will be discussed in a future publication.

Acknowledgments

This work was supported by NASA Grant #NAGW-81, and one of us (K.P.) was also supported by ONR N00014 79C 0665.

References

Auer, P. L., R. W. Kilb, and W. F. Crevier, Thermalization of the earth's bow shock, *J. Geophys. Res.*, **76**, 2927, 1971.

- Bame, S. J., J. R. Asbridge, J. T. Gosling, M. Halbig, G. Paschmann, N. Sckopke, and H. Rosenbauer, High temporal resolution observations of electron heating at the bow shock, *Space Sci. Rev.*, **23**, 75, 1979.
- Biskamp, D. and H. Welter, Numerical studies of magnetosonic collisionless shock waves, *Nucl. Fusion*, **12**, 663, 1972.
- Chodura, R. A hybrid fluid-particle model of ion heating in high Mach-number shock waves, *Nucl. Fusion*, **15**, 55, 1975.
- Davidson, R. C. and N. A. Krall, Anomalous transport in high temperature plasma with application to solenoidal fusion systems, *Nucl. Fusion*, **17**, 1313, 1977.
- Forslund, D. and J. P. Freidberg, Theory of laminar collisionless shocks, *Phys. Rev. Lett.*, **27**, 1189, 1971.
- Greenstadt, E. W. and R. W. Fredricks, Shock system in collisionless space plasmas, in *Solar System Plasma Physics*, Volume III, edited by Lanzerotti, C. F. Kennel and E. N. Parker, p. 3, North-Holland Publishing Company, 1979.
- Heppner, J. P., M. Sugiura, T. L. Skillman, B. G. Ledley, and M. Campbell, OGO-A magnetic field observations. *J. Geophys. Res.*, **72**, 5417, 1967.
- Mason, R. J., Ion and electron pressure effects on magnetosonic shock formation, *Phys. Fluids*, **15**, 1082, 1972.
- Morse, D. L., A model for ion thermalization in the Earth's bow shock, *J. Geophys. Res.*, **81**, 6126, 1976.
- Papadopoulos, K., C. E. Wagner, and I. Haber, High-mach-number turbulent magnetosonic shocks, *Phys. Rev. Lett.*, **27**, 982, 1971.
- Paschmann, G., N. Sckopke, G. Haerendel, S. J. Bame, J. R. Asbridge, and J. T. Gosling, *EOS*, **AGU**, **62**, 363, 1981.
- Russell, C. T. and E. W. Greenstadt, Initial ISEE magnetometer results: shock observations, *Space Sci. Rev.*, **23**, 3, 1979.
- Russell, C. T., M. M. Hoppe, and W. A. Livesey, Overshoots in planetary bow shocks, IGPP, University of California, Institute Publication No. 2182, 1981.
- Sgro, A. G. and C. W. Nielson, Hybrid model studies of ion dynamics and magnetic field diffusion during pinch implosions, *Phys. Fluids*, **19**, 126, 1976.
- Sherwell, D. and R. A. Cairns, Ion dynamics in a perpendicular collisionless shock, *J. Plasma Phys.*, **17**, part 2, 265, 1976.
- Tidman, D. A., and N. A. Krall, Shock waves in collisionless plasmas, John-Wiley-Interscience, New York, 1971.

(Received July 15, 1981;
revised September 15, 1981;
accepted October 16, 1981.)